Available online at www.sciencedirect.com
ScienceDirect
International Journal of Thermal Sciences 46 (2007) 755–767
International Journal of Thermal Sciences
www.elsevier.com/locate/ijts

Modeling and analysis of combustion assisted thermal spray processes

Tariq Shamim *, Chunmei Xia, Pravansu Mohanty

Department of Mechanical Engineering, The University of Michigan–Dearborn, Dearborn, MI 48128-1491, USA

Received 27 June 2006; received in revised form 13 October 2006; accepted 16 October 2006

Available online 20 November 2006

Abstract

The combustion assisted thermal spray systems are being used to apply coatings to prevent surface degradation. They offer a highly attractive way to modify the surface properties of the substrate to extend the product life. In addition to the materials being sprayed, the quality of combustion assisted thermal spray coating depends greatly on the flow behavior of reacting gases and particle dynamics. The present study investigates the effect of gas phase and its interaction with particles through the nozzle of a thermal spray gun by developing a comprehensive mathematical model. The objective is to develop a predictive understanding of various design parameters of combustion assisted thermal spray systems. The model was developed by considering the conservation of mass, momentum and energy of reacting gases. The particle dynamics was decoupled from the gas phase dynamics since the particle loading in the spray process is very low. The developed model was employed to investigate the influence of various design parameters on the coating quality of thermal spray process.

Keywords: Thermal spray; High velocity oxy-fuel; Coating; Simulations

1. Introduction

Combustion assisted thermal spray processes have been widely used in many applications including aerospace, automotive, power generation industries, and many others [1–6]. They are mainly used to improve the material surface properties, such as roughness and thermal resistance, and to rebuild the worn components. These spraying techniques use the thermal energy produced by the combustion of fuel with oxygen to heat and propel the particles. There has been an increasing interest in the combustion based thermal spray processing in recent years motivated by several factors, including:

(i) Combustion based thermal spray processes provide an efficient way for depositing coatings of nanostructured materials [7];
(ii) the powder particles hit the substrate with relatively high speed, which produces coatings with high density and high hardness; and
(iii) relatively low gas temperature prevents particles from being superheated during flight and helps to preserve the nanocrystalline/amorphous structure of deposits [8].

However, the combustion assisted processes are not free from problems and many application difficulties exist. For example, a considerable amount of carbon and oxygen can be picked up from the combustion gases, which may result in severe brittleness. Therefore, it is necessary to control the combustion products or in turn understand the combustion process itself for utilizing materials that are chemically sensitive. Such problems are also encountered in nanostructured material deposition due to high surface reactivity of fine powders.

In addition to the materials being sprayed, the quality of combustion assisted thermal spray coating depends greatly on the flame characteristics including its temperature, location, shape and emissions generated. For the best coating quality, the combustion chamber of the spray gun system must burn a stoichiometric mixture generating a predefined temperature. Any excess amount of fuel (rich mixture) will result in the generation of soot and other particulate which will contaminate the coating. Similarly, an excess amount of air (lean mixture), which will result in unburned air, will also contaminate the coat-

* Corresponding author. Tel.: +1(313) 593 0913; fax: +1(313) 593 3851.
E-mail address: shamim@umich.edu (T. Shamim).

1290-0729/$ – see front matter
doi:10.1016/j.ijthermalsci.2006.10.005

Nomenclature

A_{ebu}	empirical coefficient in eddy breakup model
A_p	particle cross-sectional area
B_{ebu}	empirical coefficient in eddy breakup model
c	turbulent model constant
C_D	drag coefficient
C_p	specific heat at constant pressure
d_p	particle diameter
$\vec{F}$	external force
h_c	convective heat transfer coefficient
H	overall enthalpy
k	turbulent kinetic energy
m_p	mass of particle
Nu	Nusselt number
p	gas pressure
P_k	production rate of turbulent kinetic energy
Pr	Prandtl number
R	gas constant
R_F	volumetric fuel consumption rate
Re	Reynolds number
S	source term
t	time
T	temperature
u_i	velocity in the i-direction
$\vec{U}$	instantaneous gas velocity vector
x_i	spatial coordinate in the i-direction

Greek variables

ε	rate of turbulent kinetic energy dissipation
λ	thermal conductivity
μ	molecular viscosity
μ_{eff}	effective viscosity
Γ_k	diffusion coefficient of k
Γ_ε	diffusion coefficient of ε
ρ	density
σ	turbulent model constant

Subscripts

F	fuel
g	gas
O	oxidant
p	particle
P	combustion product
t	turbulent

ing by oxidation. The effect of the flame location and shape on the coating quality can be controlled by accurately monitoring the flow rate and ensuring flow uniformity through all nozzles. In addition to a deteriorating coating quality, the partial blocking of some nozzles will also result in localized high temperatures which may eventually cause the meltdown of combustion chamber of the spray gun. To avoid such a catastrophe and poor coating quality requires the continuous monitoring and control of the physical and chemical processes occurring in the thermal spray system. This requires good fundamental understanding of these processes.

The microstructure and physical properties of the coatings are highly dependent on the momentum and thermal history of particles impinging on a substrate and the size distribution of the particles. These, in turn, are determined by the gas phase dynamics and a large number of parameters such as the spray gun design (which is typically a converging-diverging nozzle), the fuel/oxygen ratio, the gas jet formation, the position of substrate in relation to the gun, the particle size, shape, materials, and injection method, etc.

Modeling can play an important role in gaining insight on these processes. Modeling can also assist in the design and development of efficient combustion assisted thermal spraying system, and can serve as a cost-effective tool for the design optimization. Over the last decade, the need to optimally design and operate thermal spray processes has motivated significant research on the development of fundamental mathematical models to explicitly account for the various physicochemical phenomena and to describe the dynamic behavior of various process components.

The processes in the spray gun are complex and involve two-phase (gas and liquid or solid particles) turbulent flow, heat transfer, chemical reactions, and supersonic/subsonic flow transitions [9]. The simulation of combustion assisted thermal spray processes mainly involves three parts: modeling of gas flow field, modeling of in-flight particle behavior, and modeling of particle impact and coating formation. Since the particle loading in these systems is generally very low, it can be assumed that the presence of particles will have negligible effect on the gas velocity and temperature. This allows the decoupling of particle and gas field. Therefore, all the three parts can be modeled separately. Some of the previous combustion assisted thermal spray modeling work focused only on the particle behavior by assuming a known gas velocity and temperature [10–12]. Other modeling approaches considered both the gas phase and particle behavior by decoupling the gas field and the particle dynamics [6,9,13]. Some other studies considered the simulation of particle impact and deformation and coating formation [14–18]. However, the use of modeling in gaining a predictive understanding of various design and operating parameters of combustion assisted thermal spray systems has received little attention. Cheng et al. [9] conducted a comprehensive study to investigate the effect of various design parameters on the performance of thermal spray systems. However, they only considered the gas phase dynamics and did not include the interaction of gas phase on the particle dynamics. Furthermore, they employed a very simplified chemical mechanism, which consisted of a single-step and infinitely fast reaction rate.

The current work is motivated by recognizing the voids in the published literature, particularly in the area of model based

optimization of combustion assisted thermal spray systems. It conducts a numerical investigation of the influence of various design and operating parameters on the performance of combustion assisted thermal spray systems. The mathematical model employed in this investigation includes the gas phase and the particle dynamics, and a multi-step chemical mechanism with finite reaction rates.

2. Mathematical formulation

The mathematical model is developed by decoupling the gas flow and particle fields. This allows solutions of gas phase and particle phase separately. The modeling of the gas flow field in the gun barrel and in the free jet involves the consideration of conservation of mass, momentum and energy, with turbulence and chemical kinetics. The resolved gas velocity and temperature will be used for the modeling of particle behavior, which involves the tracking of particle velocity, position, temperature, and size distribution. The flow chart of modeling approach is shown in Fig. 1.

Eulerian formulation and ideal gas assumption are used for the gas phase to solve the high speed, compressible, Newtonian flow. Lagrangian formulation is used for the particle phase. The present study considers a single particle tracking. The effect of multiple particles and size distribution will be considered in a future study. Since the spray gun is axisymmetric, a two-dimensional domain was considered, as shown in Fig. 2.

2.1. Gas phase dynamics

The governing equations for the gas phase were developed by considering the conservation of mass, momentum and energy. The turbulence effects were modeled by using a k–ε model. The resulting governing equations are listed below:

Continuity:

$$\frac{\partial \rho}{\partial t} + \frac{\partial (\rho u_j)}{\partial x_j} = 0 \tag{1}$$

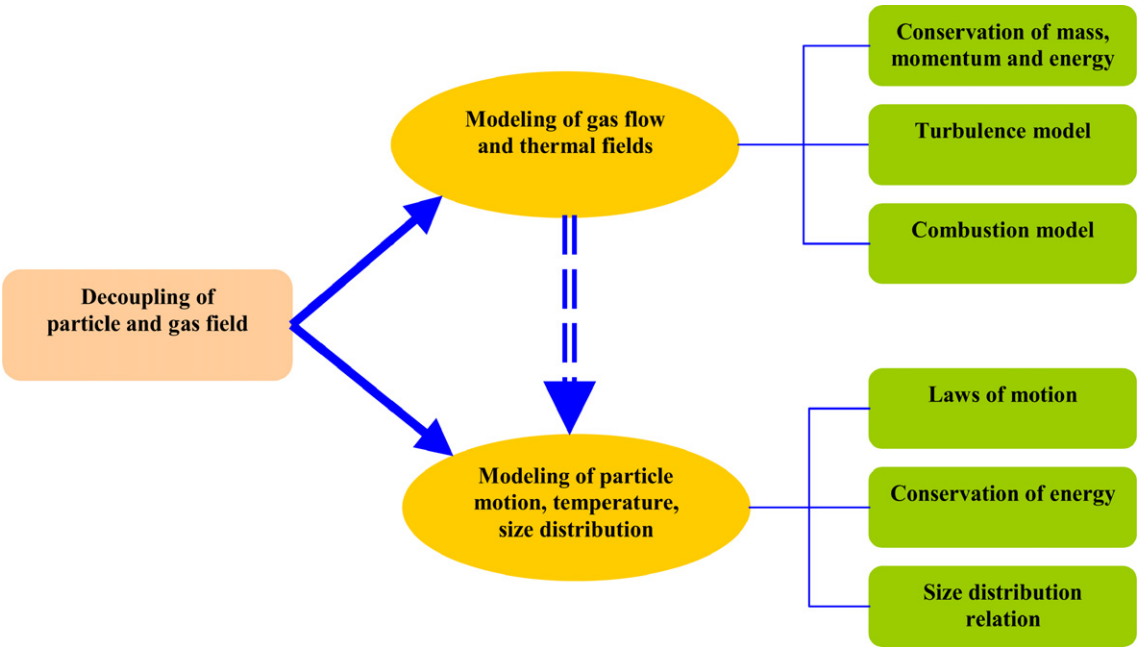

Fig. 1. Flow chart of modeling approach.

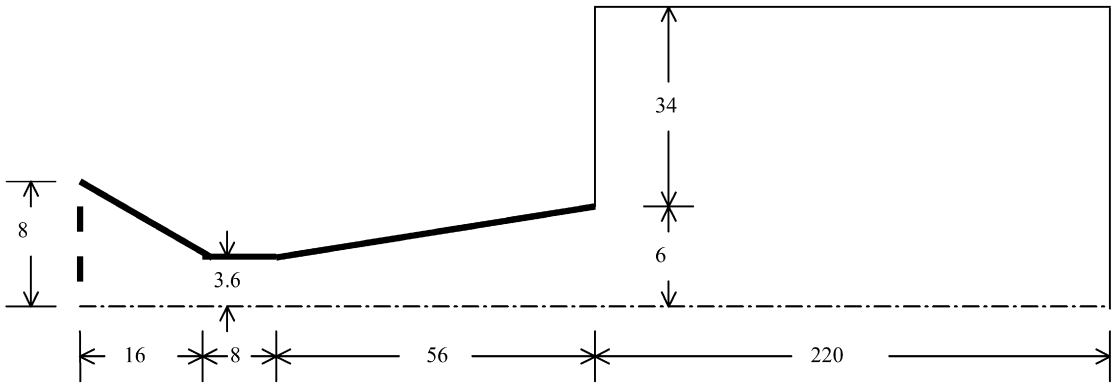

Fig. 2. Geometry of the spray gun system (dimensions in mm).

Momentum:

$$\frac{\partial}{\partial t}(\rho u_i) + \frac{\partial}{\partial x_j}(\rho u_j u_i) = -\frac{\partial p}{\partial x_i} + S_{u_i} + \frac{\partial}{\partial x_j}\left\{\mu_{\text{eff}}\left(\frac{\partial u_i}{\partial x_j} + \frac{\partial u_j}{\partial x_i}\right) - \frac{2}{3}\mu_{\text{eff}}\frac{\partial u_l}{\partial x_l}\delta_{ij}\right\} \tag{2}$$

Energy:

$$\frac{\partial}{\partial t}(\rho H) + \frac{\partial}{\partial x_j}(\rho u_j H) - \frac{\partial p}{\partial t} = \frac{\partial}{\partial x_j}\left(\lambda\frac{\partial T}{\partial x_j} + \frac{\mu_t}{\text{Pr}_t}\frac{\partial h}{\partial x_j}\right) + S_E + \frac{\partial}{\partial x_j}\left\{u_j\left[\mu_{\text{eff}}\left(\frac{\partial u_i}{\partial x_j} + \frac{\partial u_j}{\partial x_i}\right) - \frac{2}{3}\mu_{\text{eff}}\frac{\partial u_l}{\partial x_l}\delta_{ij}\right] + \mu\frac{\partial k}{\partial x_j}\right\} \tag{3}$$

Equation of state:

$$p = \rho RT \tag{4}$$

where

$$\mu_{\text{eff}} = \mu + \mu_t \quad \text{(effective viscosity)} \tag{5}$$

$$\mu_t = \rho c_\mu \frac{k^2}{\varepsilon} \quad \text{(eddy viscosity)} \tag{6}$$

$$H = h + \frac{1}{2}(u_i u_i) + k \quad \text{(overall enthalpy)} \tag{7}$$

k–ε turbulence model:

Turbulent kinetic energy:

$$\frac{\partial}{\partial t}(\rho k) + \frac{\partial}{\partial x_j}(\rho u_j k) = \frac{\partial}{\partial x_j}\left(\Gamma_k\frac{\partial k}{\partial x_j}\right) + P_k - \rho\varepsilon \tag{8}$$

Rate of turbulent kinetic energy dissipation

$$\frac{\partial}{\partial t}(\rho\varepsilon) + \frac{\partial}{\partial x_j}(\rho u_j \varepsilon) = \frac{\partial}{\partial x_j}\left(\Gamma_\varepsilon\frac{\partial \varepsilon}{\partial x_j}\right) + \frac{\varepsilon}{k}(c_1 P_k - \rho c_2 \varepsilon) \tag{9}$$

where Γ_k and Γ_ε represent diffusion coefficients of k and ε respectively. They are expressed as:

$$\Gamma_k = \mu + \frac{\mu_t}{\sigma_k} \tag{10}$$

and

$$\Gamma_\varepsilon = \mu + \frac{\mu_t}{\sigma_\varepsilon} \tag{11}$$

P_k represents the production rate of turbulent kinetic energy and is determined as:

$$P_k = \mu_t\left(\frac{\partial u_i}{\partial x_j} + \frac{\partial u_j}{\partial x_i}\right)\frac{\partial u_i}{\partial x_j} - \frac{2}{3}\left(\rho k + \mu_t\frac{\partial u_l}{\partial x_l}\right)\frac{\partial u_k}{\partial x_k} \tag{12}$$

The following values were used for the constants: $c_1 = 1.44$, $c_2 = 1.92$, $\sigma_k = 1.0$, $\sigma_\varepsilon = 1.3$, and $c_\mu = 0.09$.

Combustion:

The combustion of fuel (propylene) was modeled by using the following 4-step kinetic mechanism:

$$C_3H_6 + 0.5O_2 \rightarrow 3CO + 3H_2 \tag{13}$$

$$CO + 0.5O_2 \rightarrow CO_2 \tag{14}$$

$$H_2 + 0.5O_2 \rightarrow H_2O \tag{15}$$

$$H_2O + 0.5O_2 \rightarrow 2OH \tag{16}$$

To consider the interaction between eddy motion and chemical reaction, the eddy break up model was used to express the reaction rate [19]. This model provides a general concept for treating the interaction between turbulence and chemistry in flames. The model assumes that the reactions are completed at the moment of mixing, so that the reaction rate is completely controlled by turbulent mixing. According to the eddy break-up model, the volumetric 'fuel' consumption rate is given by:

$$R_F = -\frac{\rho\varepsilon}{k}A_{\text{ebu}}\min\left[m_F, \frac{m_O}{s_O}, B_{\text{ebu}}\frac{m_P}{s_P}\right] \tag{17}$$

where

$$s_O \equiv n_O M_O / n_F M_F \tag{18}$$

$$s_P \equiv n_P M_P / n_F M_F \tag{19}$$

Here A_{ebu} and B_{ebu} are empirical coefficients with normal default values 4 and 0.5, respectively. The subscript F, O and P represent fuel, oxidant and products, respectively.

2.2. Particulate phase dynamics

The particle trajectories and temperature histories in the gas field are computed by the momentum and heat transfer equations. Because the acceleration and deceleration of particles in the moving gas in the combustion assisted thermal spray system are dominated by the drag force, the particle motion can be described by the following ordinary differential equations

$$m_p\frac{d\vec{V}_p}{dt} = \frac{1}{2}\rho_g A_p C_D(\vec{U}_g - \vec{U}_p)|\vec{U}_g - \vec{U}_p| + \vec{F} \tag{20}$$

Here m_p is the mass of particle, $\vec{U}_p$ and $\vec{U}_g$ are instantaneous particle and gas velocities, ρ_g is gas density, A_p is particle cross-sectional area, $\vec{F}$ represents the external forces, and C_D is drag coefficient, which is modeled by the following correlation:

$$C_D = \begin{cases} 24(1 + 0.15Re_p^{0.687})/Re_p, & Re_p \leqslant 10^3 \\ 0.44, & Re_p > 10^3 \end{cases} \tag{21}$$

where

$$Re_p = \rho_g\frac{|\vec{U}_g - \vec{U}_p|}{\mu_g}d_p \tag{22}$$

Here, μ_g is the viscosity of the gas and d_p is the particle diameter.

In the spray process, the particle Biot number is typically less than 0.1 [20]. This means that particles are heated with negligible internal resistance and the temperature gradients inside the particles can be ignored. Consequently, the equation describing the heat transfer between a single particle and the

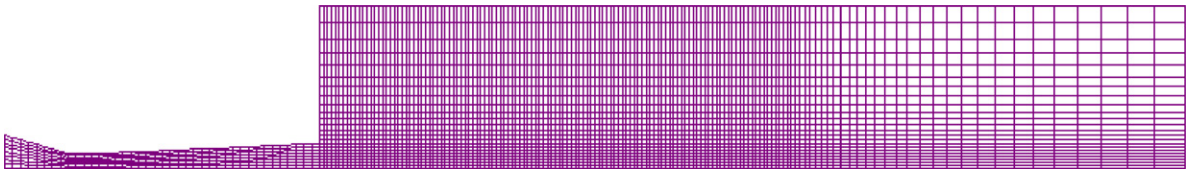

Fig. 3. Computational mesh.

gas reduces to a first-order ordinary differential equation of the form:

$$m_p C_p \frac{dT_p}{dt} = A_p h_c (T_g - T_p) \tag{23}$$

where C_p is the specific heat of the particle and h_c is convective heat transfer coefficient, which is defined as:

$$h_c = \frac{Nu\,\lambda}{d_p} \tag{24}$$

where Nu is the Nusselt number, which is obtained from the following correlation proposed by Ranz and Marshall [21]:

$$Nu = 2.0 + 0.6 Pr^{0.33} Re^{0.5} \tag{25}$$

2.3. Boundary conditions and computational domain

There are three inlets at the nozzle inlet. All gas inlet temperatures are assumed to be at 293 K. The walls are smooth and adiabatic. The pressure is assumed to be 1 atm at open boundaries. The chemical mechanism considered seven gas species: C_3H_6, O_2, CO, H_2, CO_2, H_2O, N_2, as in Ref. [6]. The values of solid particle diameter, specific heat and density were: $d_p = 15\ \mu m$, $C_p = 450\ J\,kg^{-1}\,K^{-1}$, $\rho_p = 7900\ kg\,m^{-3}$.

The computational domain, as shown in Fig. 3, consists of 80×8 grids inside the gun barrel and 150×23 grids outside the barrel. In the horizontal direction, the outside mesh included 120 uniform grids for the first 120 mm followed by 30 stretched grids. The outside mesh in the vertical direction included 8 uniform grids for the first 6 mm followed by 15 stretched grids.

3. Model validation

Using the current gas phase and particle tracking model, the results for particle temperature and velocity were compared with the numerical and experimental results of Ref. [6], as shown in Fig. 4. The nozzle exit is located at an axial distance of 80 mm. The flow rates of reactants, coolant and carrier gas, the fuel/oxygen ratio, and the particle properties were setup according to the conditions of Ref. [6]. The figure shows that the particle temperature and velocity from the current model are close to the numerical results of Ref. [6] inside the nozzle and right after the nozzle exit. The current model also simulates the experimental results more accurately than the numerical results of Ref. [6] at the farther part of the domain.

4. Results and discussion

The model is employed to investigate the influence of various design parameters on the performance of thermal spray system. The following sections describe the effects of some of the important parameters.

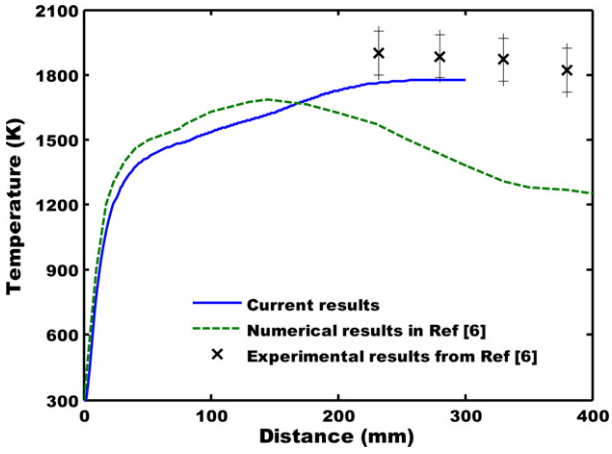

(a)

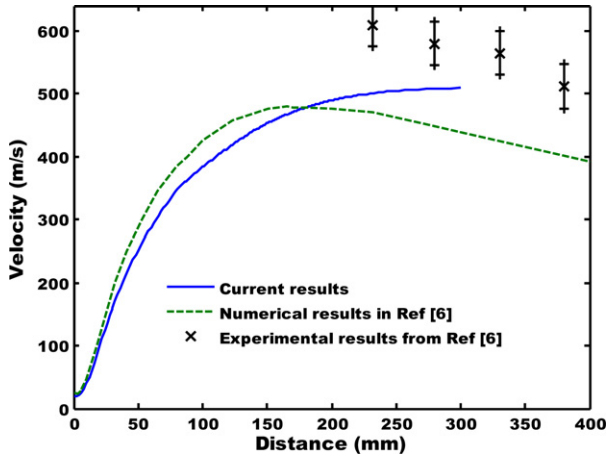

(b)

Fig. 4. Comparison with experimental and previous numerical results for (a) particle temperature and (b) particle velocity variation with distance.

4.1. Effects of the reactant mass flow rate

The reactant mass flow rate has significant effects on the gas phase and particle properties, as shown in Fig. 5. The increase in reactant mass flow rate increases the total mass flow rate, which causes an increase in gas pressure (as evident from ideal gas equation). Along the diverging section of the nozzle, the gas mixture achieves supersonic speed and the pressure at the nozzle exit drops to below atmospheric for all cases. This results in shock waves at the exit. Since the exit pressure is lower for lower reactant mass flow rate cases, the pressure jumps are relatively higher for these cases, however, they reach at the equilibrium value (ambient pressure) faster. The increase in reactant mass flow rate decreases the fluctuation amplitude but increases the time to achieve equilibrium.

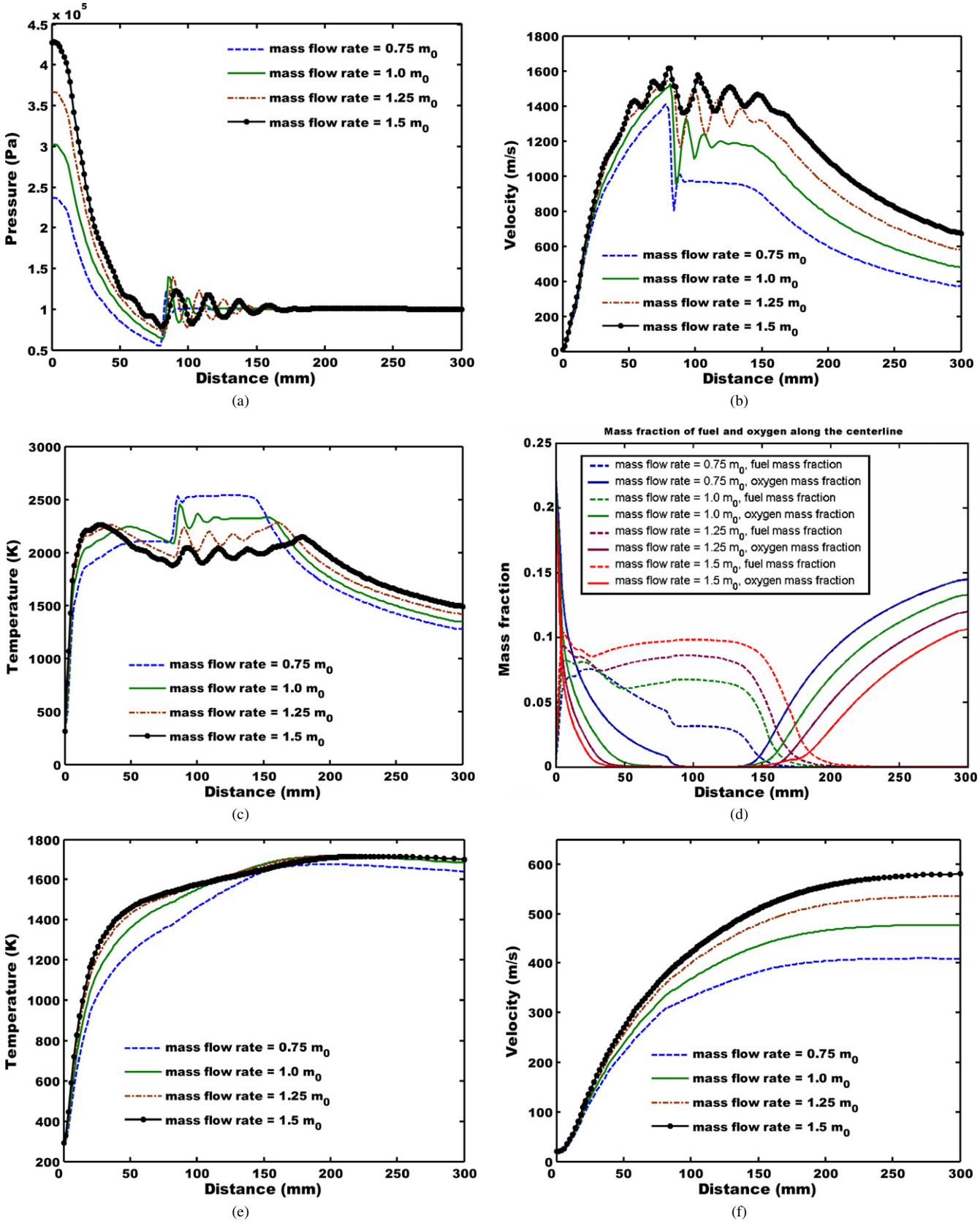

Fig. 5. Effect of reactant mass flow rate: Variation of (a) gas phase pressure; (b) gas phase velocity; (c) gas phase temperature; (d) reactant mass fractions; (e) particle temperature; and (f) particle velocity.

The gas phase temperature is also influenced by the reactant mass flow rate. The influence is different on different parts of the nozzle. This is due to the fact that the temperature is significantly influenced by combustion, which is highly dependent on the mass fraction of fuel and oxygen. The mixture is oxygen rich from the inlet up to 50 mm inside the nozzle where fuel concentration becomes the determining factor for the combustion intensity. Hence, the temperature is higher for higher mass flow rate in this region since the fuel concentration is higher. The mixture becomes oxygen lean from this region to a distance of approximately 200 mm from the nozzle inlet. In this region, the combustion rate is determined by the availability of oxygen. Consequently, the temperature is lower for higher mass flow rate in this region. At the nozzle exit, the temperature profile undergoes a jump owing to shock waves. The amplitude of temperature jump decreases with an increase of reactant mass flow rate. At a distance farther from the nozzle exit, the ambient oxygen penetrates to the centerline from outside and reacts with the existing fuel. This results in higher temperature for the higher reactant mass flow rate case.

The gas phase velocity increases with an increase of reactant mass flow rate. For all cases, the velocity continuously increases along the nozzle and is at its peak value at the nozzle exit. The effect of reactant mass flow rate is negligibly small in the converging section of the nozzle but becomes gradually significant along the diverging section. At the exit, owing to shock waves, the velocity profile undergoes a jump for all cases. The amplitude of velocity jump is higher at lower reactant mass flow rate, which experiences a greater pressure increase. Similar to pressure profile, the velocity profile of lower reactant mass flow rate case reaches at the equilibrium value faster.

The reactant mass flow rate also affects the particle temperature and velocity. The particle temperature increases with an increase of reactant mass flow rate and the corresponding increase of gas temperature. The effect is more significant near the nozzle exit. Note that the particle temperature does not follow the gas temperature's decreasing trend near the nozzle exit. This can be explained by considering that the particle is at much lower temperature than the gas phase, and hence, it still gets heated when the gas phase is losing temperature. The particle reaches its peak outside of the nozzle. After reaching the peak value, the particle experiences some temperature drop. At this point, the reactant mass flow rate does not have any appreciable effect on the particle temperature. The increase of reactant mass flow rate also increases the particle velocity. The increase is owing to corresponding higher gas phase velocity, which provides a better convection environment for accelerating the particle. The effect is greater outside of the nozzle.

4.2. Effects of the mass flow rate of coolant

The variation in coolant mass flow rate also affects the gas phase and particle properties, as shown in Fig. 6. Its effect on the gas phase pressure is similar to that of the reactant mass flow rate. An increase in coolant mass flow rate increases the total mass flow rate, which, in turn, causes an increase in gas pressure. As expected, the increase in coolant flow rate decreases the gas phase temperature in the initial part of the nozzle. For all cases, the temperature reaches a peak value in the diverging section of the nozzle. However, in this part of the nozzle, the temperature is lower for less cooling flow rate case. This can be explained by considering that less coolant mass flow rate case has lower thermal inertia and, hence, loses heat relatively faster than that of the high coolant mass flow rate case. Outside of the nozzle, the coolant has sufficient time to penetrate to the center and, hence, the temperature is lower for higher coolant flow rate. Overall, the effect of coolant flow rate inside the nozzle is small, which is due to the fact that the coolant is injected above the centerline and it does not immediately penetrate to the center of the spray domain. Hence, the centerline velocity and temperature profiles, shown in Figs. 6(b) and 6(c), exhibit little effect of varying coolant flow rate.

However, the variation in coolant flow rate has much greater effect near the coolant inlet, for example, along an upper line at $y = 3$ mm. In this case, an increase in coolant flow rate decreases the gas phase temperature inside and outside of the nozzle. An increase of coolant flow rate shifts the location of the peak temperature away from the nozzle inlet. For some cases, there are small temperature jumps inside the nozzle, which are initiated at locations within the reaction zone, where the rate of cooling is faster than the rate of heat released for a short period of time. For all coolant mass flow rates, the gas phase velocity profiles show similar trends. Near the nozzle inlet (up to 20 mm), the centerline velocity is not much affected by the coolant flow rate. Further along the length, the velocity increases with a decrease of coolant mass flow rate. Similar to the effect of reactant mass flow rate, the velocity jump at the nozzle exit is larger for lower coolant mass flow rates. The effect of coolant mass flow rate on the velocity profiles near the coolant injection location are similar but stronger.

The coolant mass flow rate does not have any significant effects on the particle temperature and velocity inside the nozzle. Outside of the nozzle, an increase of coolant flow rate decreases the particle temperature and increases its velocity.

4.3. Effects of fuel/oxygen ratio

Fig. 7 shows that the fuel/oxygen (F/O) ratio has significant effect on both the gas phase and particle. The increase in F/O ratio increases the gas phase pressure near the nozzle inlet. The increase is greater at the lower values of F/O ratio and gradually becomes smaller. There is no significant difference in pressure values for F/O ratios of 0.3 and 0.35 (rich mixture). The pressure profile does not follow the same trend throughout the nozzle length. Near the nozzle exit, the pressure values of F/O ratios of 0.3 and 0.35 fall below that of the F/O ratio of 0.25 (lean mixture). At the nozzle exit, the pressure is below atmospheric and the shock waves exist for all the F/O ratio cases. The pressure jump is higher and the fluctuations in the pressure profile last longer for higher values of F/O ratios.

The effects of F/O ratio on the gas phase temperature are similar to the effects of reactant mass flow rate, because the temperature is influenced by combustion, which is highly dependent on the availability of fuel and oxygen. The results show

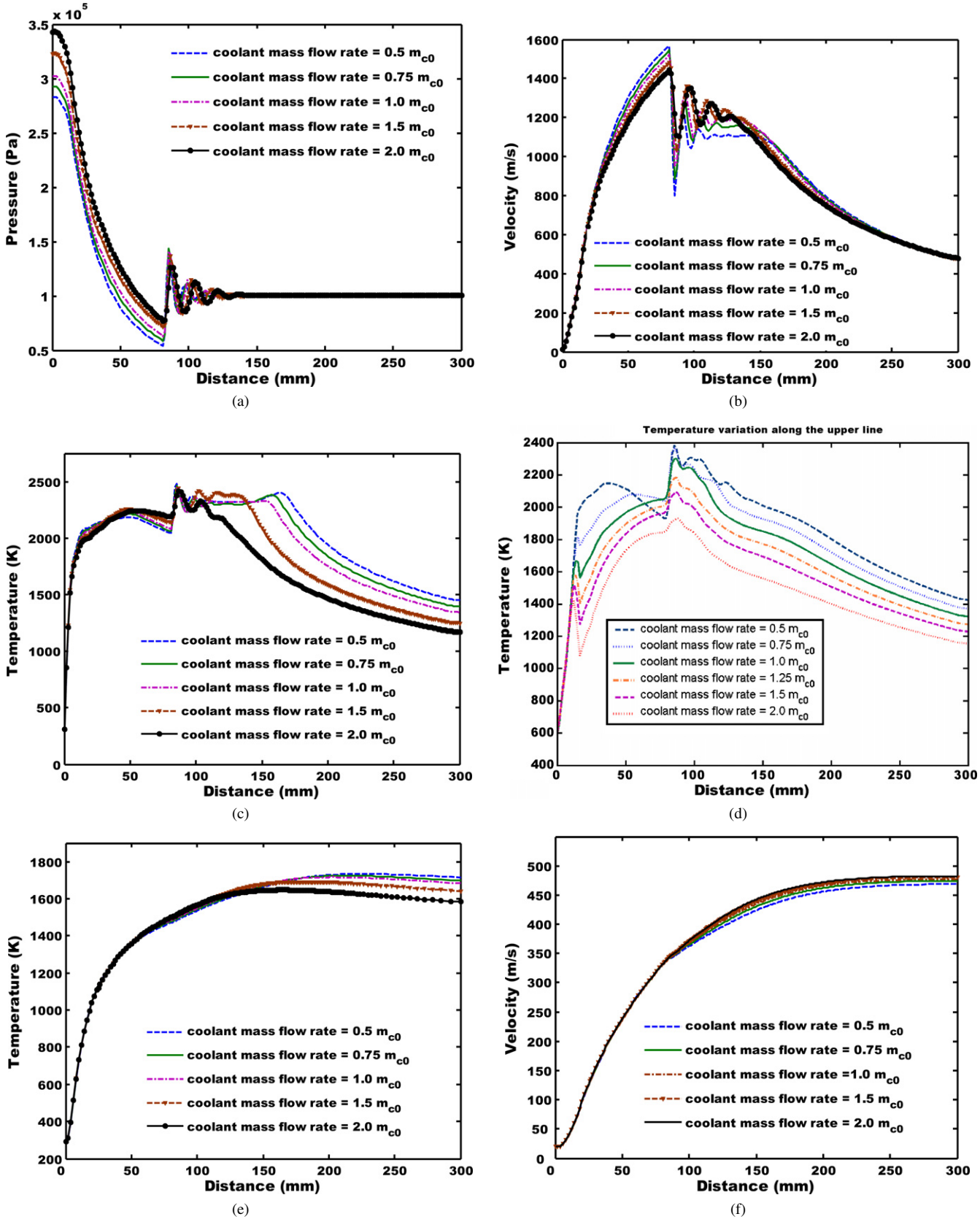

Fig. 6. Effect of coolant mass flow rate: Variation of (a) gas phase pressure; (b) gas phase temperature along the centerline; (c) gas phase velocity along the centerline; (d) gas phase temperature along an upper line; (e) particle temperature; and (f) particle velocity.

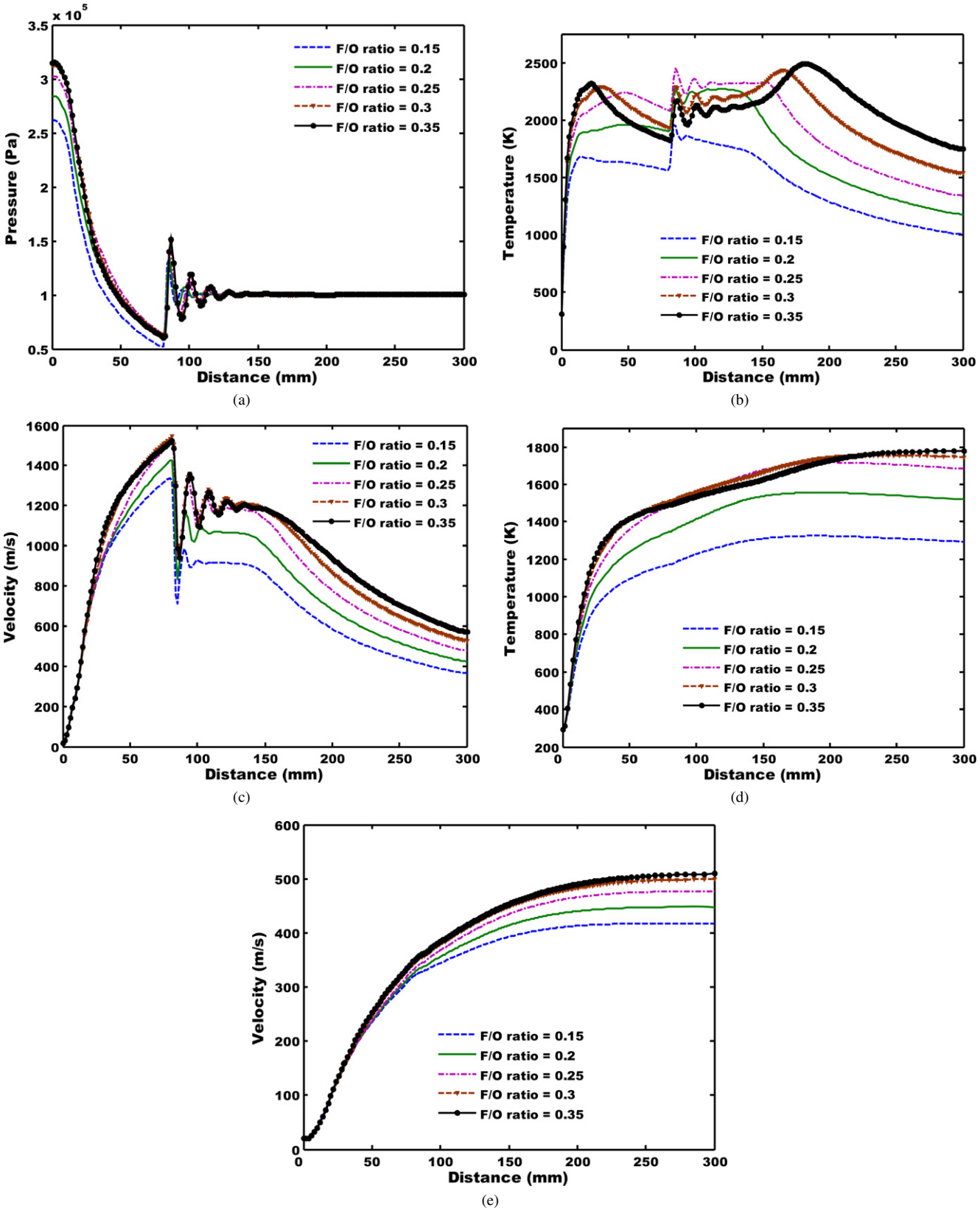

Fig. 7. Effect of fuel/oxygen ratio: Variation of (a) gas phase pressure; and (b) gas phase velocity; (c) gas phase temperature; (d) particle temperature; and (e) particle velocity.

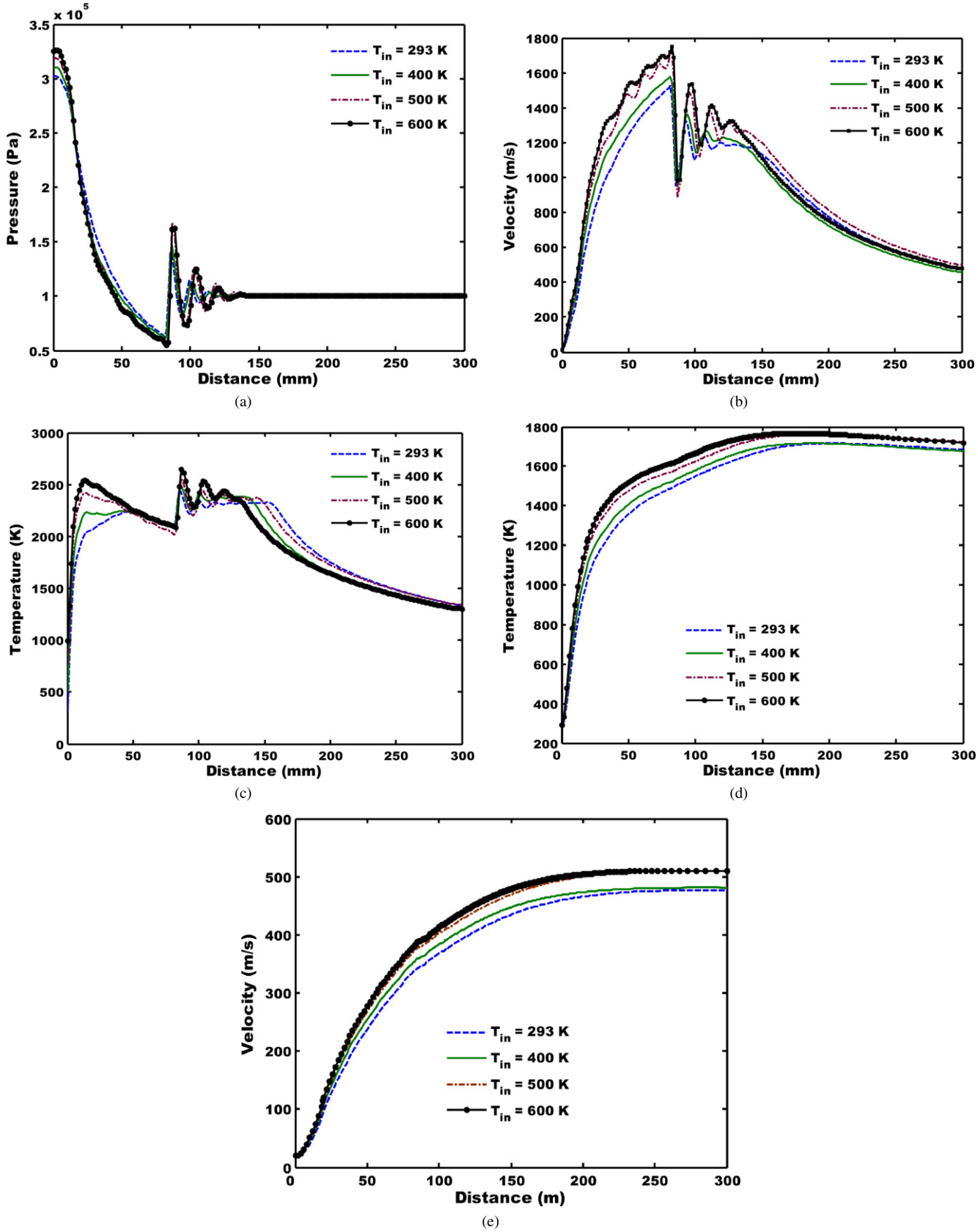

Fig. 8. Effect of preheating of the reactants: Variation of (a) gas phase pressure; and (b) gas phase velocity; (c) gas phase temperature; (d) particle temperature; and (e) particle velocity.

that the temperature peak inside the nozzle increases with an increase of F/O ratio. For F/O ratio below stoichiometric value ($\sim$0.29), an increase in F/O ratio shifts the peak temperature location away from the nozzle inlet. The peak temperature location starts moving back toward the nozzle inlet as the F/O ratio is increased beyond the stoichiometric value. The effect of F/O ratio on the gas temperature at the nozzle exit also depends on whether it is lean or rich mixture. For the lean mixture (F/O ratio < 0.29), an increase in F/O ratio increases the exit temperature, whereas, an increase in F/O ratio decreases the exit temperature for a rich mixture (F/O ratio > 0.29). The rich cases (F/O ratios of 0.3 and 0.35) have additional amount of unburned fuel at the nozzle exit, which burns with the outside air. Consequently, outside of the nozzle, the rich cases have higher peak temperatures.

The gas phase velocity increases throughout the nozzle, with the peak value occurring at the exit. The velocity is similar for different F/O ratios near the nozzle inlet (up to approximately 20 mm length). The effect of F/O ratio becomes important after the combustion is initiated. After that, an increase of F/O ratio results in an increase in the velocity for lean mixtures and a decrease for rich mixtures. Outside of the nozzle, the velocity increases with an increase of F/O ratio for both lean and rich mixtures. The increase in velocity for rich mixtures is due to higher temperatures of higher F/O ratio cases, as explained earlier.

The variation in gas phase temperature and velocity caused by F/O ratio variation also affects the particle temperature and velocity. The effects are relatively higher at low F/O ratios and become gradually smaller at higher F/O ratios. The increase of F/O ratio generally increases the particle temperature and velocity. The increasing effect is low near the nozzle inlet and it becomes gradually more significant in the diverging section of the nozzle. Inside the nozzle, the particle temperature follows the trend of gas phase temperature closely and the effect of F/O ratio is different for lean and rich mixtures. Outside of the nozzle, the particle temperature increases with an increase of F/O ratio for both lean and rich mixtures. The effects of F/O ratio on the particle velocity are similar.

4.4. Effects of preheating of the reactants

The effect of preheating of reactants was investigated by varying the reactant temperature from 293 K to 600 K, and the results are plotted in Fig. 8. The preheating increases the gas pressure at the nozzle inlet. Higher preheating also causes larger pressure drop inside the nozzle, which results in lower pressure and, consequently, larger pressure jump at the nozzle exit for the higher preheating case. The preheating of reactants increases the burning rate and, hence, the peak gas phase temperature inside the nozzle is increased, but it does not have any significant effect on the temperature at the nozzle exit. The peak temperature location shifts towards the nozzle inlet when the reactants are preheated from 293 K to 400 K. Further preheating does not affect the peak temperature location. Outside of the nozzle, the preheating results in larger fluctuations of temperature. After temperature fluctuations cease to exist, the temperature is higher for lower preheating case. This is due to availability of relatively larger amount of unburned fuel, which burns with the outside air.

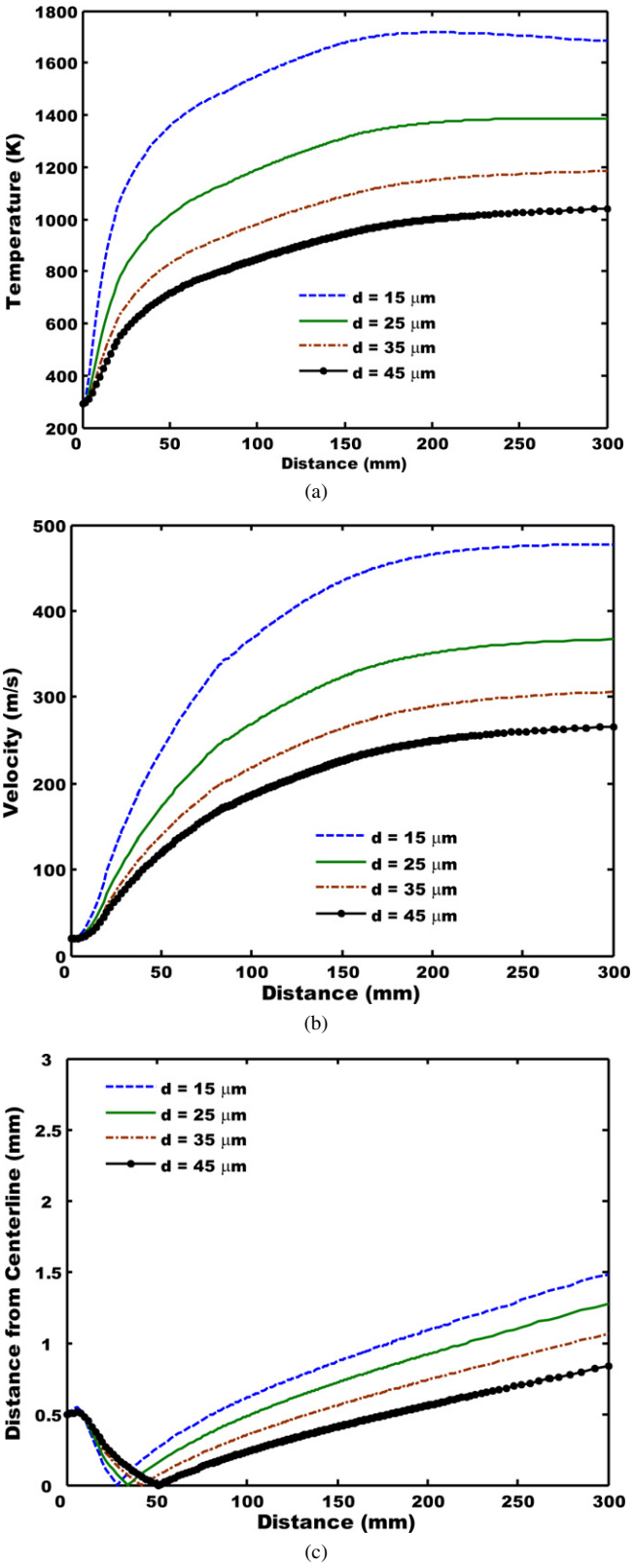

Fig. 9. Effect of particle size: Variation of particle (a) temperature; (b) velocity; and (c) trajectories.

The gas phase velocity increases with an increase of preheating throughout the nozzle length. The effect of preheating becomes gradually stronger along the nozzle. The preheating at higher temperature results in velocity fluctuations inside the nozzle. Higher preheating level also results in larger velocity jump at the nozzle exit. Outside of the nozzle exit, when the fluctuations cease to exist, there is no clear trend of the effect of preheating on velocity.

The preheating does not have any significant effect on the particle temperature and velocity near the nozzle inlet. The effect becomes gradually more significant as the particle moves along the nozzle length. Overall, the preheating of reactants increases the particle temperature and velocity.

4.5. Effects of particle size

The particle properties in the thermal spray system depend greatly on the gas phase properties and the particle size and distribution. Fig. 9 presents the results of particle size with four different particle diameters: 15 μm, 25 μm, 35 μm, and 45 μm. As expected, the decrease in the particle size results in higher particle temperature and velocity, which is owing to decrease in particle thermal and mass inertia. The influence of the particle size is greater for smaller sized particles. For example, a change in the particle diameter from 25 μm to 15 μm causes an increase in the particle temperature and velocity approximately by 20% and 30% respectively. The particle trajectories show that smaller particles also move to a greater radial distance from their injection locations. The particle is injected from a location above the centerline. Immediately after the injection, the particle moves towards the center due to gravity. However, the supersonic flow inside the nozzle gradually pushes the particle away from the center. The movement of particle from its injection location is decreased with an increase in the particle diameter and the corresponding mass.

5. Conclusions

A numerical investigation was conducted to investigate the influence of various operating parameters on the performance of combustion assisted thermal spray systems. The gas phase temperature, velocity and pressure were found to depend on a series of parameters, including mass flow rate of the gas phase, fuel/oxygen ratio, reactant preheating and cooling rate. The actual effects of these parameters are different in different parts of the nozzle and the region outside of the nozzle. The local conditions, such as whether the flow is subsonic or supersonic, reacting or non-reacting, availability of reactants, etc., are important in the determination of these effects. The gas phase properties have strong influence on the particle temperature and velocity. However, the particle temperature and velocity profiles generally exhibit smoothly increasing trends along the length and do not reflect the trend changes of gas phase properties. This is due to a relatively large difference between particle and gas phase temperature and velocity values. Hence, for example, a particle does not start losing temperature when the gas phase temperature experiences a decrease since the reduced gas temperature is still significantly higher than the particle temperature. As expected, the particle size also has significant influence on its temperature and velocity.

Acknowledgements

Financial support from the US Army-TARDEC under contract number DAAE07-03-C-L148 is gratefully acknowledged.

References

[1] G.W. Goward, Protective coatings—purpose, role and design, Materials Science and Technology 2 (1986) 194–200.
[2] D.B. Meadowcroft, High temperature corrosion alloys and coatings in oil- and coal-fired boilers, Materials Science and Engineering 88 (1987) 313–320.
[3] B.Q. Wang, The dependence of erosion.corrosion wastage on carbide/metal binder proportion for HVOF carbide metal cermet coatings, Wear 196 (1996) 141–146.
[4] B.Q. Wang, K. Luer, The erosion–oxidation behavior of HVOF Cr3C2-NiCr cermet coating, Wear 174 (1994) 177–185.
[5] M. Bjordal, E. Bardal, T. Rogne, T.G. Eggen, Combined erosion and corrosion of thermal sprayed WC and CrC coatings, Surface and Coatings Technology 70 (1995) 215–220.
[6] A. Dolatabadi, J. Mostaghimi, V. Pershin, Effect of a cylindrical shroud on particle conditions in high velocity oxy-fuel (HVOF) spray process, Journal of Materials Processing Technology 137 (2003) 214–224.
[7] M.L. Lau, H.G. Jiang, W. Nuchter, E.J. Lavernia, Thermal spraying of nanocrystalline Ni coatings, Physica Status Solidi A – Applied Research 166 (1998) 257–268.
[8] D.J. Branagan, W.D. Swank, D.C. Haggard, J.R. Fincke, Wear-resistant amorphous and nanocomposite steel coatings, Metallurgical and Materials Transactions A 32 (2001) 2615–2621.
[9] D. Cheng, Xu Q., Trapaga G., Lavernia E.J., A numerical study of high-velocity oxygen fuel thermal spraying process. Part I: Gas phase dynamics, Metallurgical and Materials Transactions A 32 (2001) 1609–1620.
[10] M.L. Lau, V.V. Gupta, E.J. Lavernia, Particle behavior of nanocrystalline 316-stainless steel during high velocity oxy-fuel thermal spray, Nano-Structured Materials 12 (1999) 319–322.
[11] V.V. Sobolev, J.M. Guilemany, A.J. Martin, J.A. Calero, P. Vilarrubias, Modeling of the In-flight behavior of stainless steel powder particles in high velocity oxy-fuel spraying, Journal of Materials Processing Technology 79 (1998) 213–216.
[12] A.M. Ahmed, R.H. Rangel, V.V. Sobolev, J.M. Guilemany, In-flight oxidation of composite powder particles during thermal spraying, International Journal of Heat and Mass Transfer 44 (2001) 4667–4677.
[13] M. Li, P.D. Christofides, Modeling and analysis of HVOF thermal spray process accounting for powder size distribution, Chemical Engineering Science 58 (2003) 849–857.
[14] O. Knotek, R. Elsing, Monte Carlo simulation of the lamellar structure of thermally sprayed coatings, Surface and Coatings Technology 32 (1987) 261–271.
[15] G. Trapaga, J. Szekely, Mathematical modeling of the isothermal impingement of liquid droplets in spray processes, Metallurgical and Materials Transactions B 22 (1991) 901–914.
[16] O. Knotek, R. Elsing, Monte Carlo simulation of the lamellar structure of thermally sprayed coatings, Surface and Coatings Technology 32 (1987) 261–271.
[17] J. Mostaghimi, S. Chandra, R. Ghafouri-Azar, A. Dolatabadi, Modeling thermal spray coating processes: A powerful tool in design and optimization, Surface and Coatings Technology 163–164 (2003) 1–11.
[18] S. Kamnis, S. Gu, Numerical modelling of droplet impingement, Journal of Physics D: Applied Physics 38 (2005) 3664–3673.

[19] B.F. Magnussen, B.H. Hjertager, On mathematical modeling of turbulent combustion with special emphasis on soot formation and combustion, Proceedings of the Combustion Institute 16 (1976) 719–729.

[20] D. Cheng, Q. Xu, G. Trapaga, E.J. Lavernia, The effect of particle size and morphology on the in-flight behavior of particles during high velocity oxy-fuel (HVOF) thermal spraying, Metallurgical and Materials Transactions B 32 (2001) 525–535.

[21] W.E. Ranz, W.R. Marshall Jr, Evaporation from drops: Part 1, Chemical Engineering Progress 48 (1952) 141–146.